

Discovery of Non-peptide, Environmental Sensitive Fluorescent Probes for Imaging p53-MDM2 Interaction in Living Cell Line and Tissue Slice

Gaopan Dong, Shipeng He, Xiaojun Qin, Tingting Liu, Yan Jiang,
Xiang Li, Long Chen, Guangxi Han, Chunquan Sheng, and Minyong Li

Anal. Chem., **Just Accepted Manuscript** • DOI: 10.1021/acs.analchem.9b04551 • Publication Date (Web): 10 Jan 2020

Downloaded from pubs.acs.org on January 10, 2020

Just Accepted

“Just Accepted” manuscripts have been peer-reviewed and accepted for publication. They are posted online prior to technical editing, formatting for publication and author proofing. The American Chemical Society provides “Just Accepted” as a service to the research community to expedite the dissemination of scientific material as soon as possible after acceptance. “Just Accepted” manuscripts appear in full in PDF format accompanied by an HTML abstract. “Just Accepted” manuscripts have been fully peer reviewed, but should not be considered the official version of record. They are citable by the Digital Object Identifier (DOI®). “Just Accepted” is an optional service offered to authors. Therefore, the “Just Accepted” Web site may not include all articles that will be published in the journal. After a manuscript is technically edited and formatted, it will be removed from the “Just Accepted” Web site and published as an ASAP article. Note that technical editing may introduce minor changes to the manuscript text and/or graphics which could affect content, and all legal disclaimers and ethical guidelines that apply to the journal pertain. ACS cannot be held responsible for errors or consequences arising from the use of information contained in these “Just Accepted” manuscripts.

Discovery of Non-peptide, Environmental Sensitive Fluorescent Probes for Imaging p53-MDM2 Interaction in Living Cell Line and Tissue Slice

Gaopan Dong ^{a,†}, Shipeng He ^{b,†}, Xiaojun Qin ^a, Tingting Liu ^{a,c}, Yan Jiang ^b, Xiang Li ^a, Long Chen ^b, Guangxi Han ^a, Chunquan Sheng ^{b,*}, Minyong Li ^{a,*}

^a Department of Medicinal Chemistry, Key Laboratory of Chemical Biology (MOE), School of Pharmacy, Shandong University, Jinan, Shandong 250012, China. Tel./fax: +86-531-8838-2076; E-mail: mli@sdu.edu.cn.

^b Department of Medicinal Chemistry, School of Pharmacy, Second Military Medical University, 325 Guohe Road, Shanghai 200433, China. E-mail: shengcq@hotmail.com

^c Institute of Pharmacology, School of Pharmaceutical Sciences, Shandong First Medical University & Shandong Academy of Medical Sciences, Taian 271000, Shandong, China.

[†]Authors contributed equally to this work.

ABSTRACT: Based on the structural optimization work, probe **9-11** with practical activity and selectivity in tissue as well as living cell lines are well designed and synthesized. All the probes showed potent inhibitory and acceptable cell toxicity compared with commercially available p53-MDM2 inhibitor Nutlin-3, and can increase the protein expression level of p53 and MDM2 in A549 cell line, in particular, probe **10** and **11** can increase the protein expression level of p53 than nutlin-3. Moreover, their application in imaging and detecting wild-type p53-MDM2 protein-protein interaction have been well demonstrated in cell and tissue level. Overall, these environment-sensitive fluorescent turn-on probes are affordable and rapid in imaging, also expected for the application in target drug screening as well as in pathologic diagnosis.

Introduction

p53, a well-known tumor suppressor, plays an indispensable role in protecting living cells against harmful damage from various cellular stresses, such as DNA damage, hypoxia, oncogenic activation, telomere erosion. It also involves in eradicating the tumor cells for normal physiological condition maintenance.^{1,5} In response to stress, p53 can participate in various cellular regulation process, such as apoptosis, cell cycle, DNA damage, senescence, hypoxia, oncogenic activation and differentiation.^{3,6,7} Under normal physiological state, p53 protein has a relative low expression level and a short half-life time (about 20 min), while under the abnormal situation, p53 transforms to a latent form, which is inactive or absent for transcription, so that it needs a specific signal to reactivate and functionalize p53.³ Generally, the level of p53 protein is strictly regulated by its master regulator MDM2 (the murine double minute-2 protein) and MDMX (also called MDM4) via a negative feedback loop.⁸ The p53 gene generally promotes the expression of the MDM2 gene and increases the level of the MDM2 protein. In turn, MDM2 binds to the N-terminal domain of the p53 protein⁹ and inhibits p53 activity through three mechanisms: binding to the transactivation structure of p53 domain;^{6,10,11} translocation

of p53 out of the nucleus;¹² and the proteasome-mediated degradation of p53 triggered by MDM2 as an E3 ubiquitin ligase.^{1,2,9,13} The inhibition of p53 in malignancies is predominantly regulated by MDM2-p53 protein-protein interaction. In fact, approximately 50% of human tumors still express wild-type p53. Therefore, reactivating the function of p53 and inhibiting the function of MDM2 are very promising cancer treatment strategies.^{1,6,14}

The current treatment strategies for activating p53 are mainly gene therapy and small molecule drug therapy.¹ Compared with gene therapy, the small molecules to reactivate p53 function is affordable by most family. However, to find effective small molecule inhibitors to stop non-enzymatic protein-protein interactions is still a challenge work. Fortunately, in 1996, Kussie et al used the X-ray crystallography to find the structural basis of the p53-MDM2 protein-protein interaction (PPI).¹⁵ The crystal structure show that the MDM2-p53 interaction is mediated by MDM2, which has a well-defined hydrophobic surface pocket and could be combined with key hydrophobic residues in p53, namely Trp23, Leu26, and Phe19.⁶ When it interacted with MDM2, the p53 peptide forms an amphipathic α -helix.¹ Based on this well-defined crystal structure, provide the basis for designing non-peptides, small molecules for blocking MDM2-p53

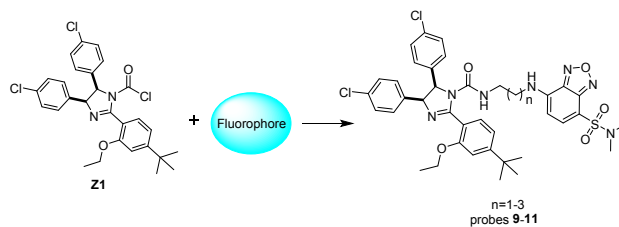
interaction and re-activating p53 function.⁶ In recent years, based on the crystal structure of MDM2-p53, there are many selective molecules having potent antitumor activity both *in vitro* and *in vivo*, such as SAR405838,¹⁶ and RG7112.^{1,17}

To better understand the interaction between p53 and MDM2, various strategies have been introduced, such as bimolecular fluorescence complementation (BiFC) assay¹⁸ and autofluorescence translocation biosensor system.^{19,20} The fluorescence technique can directly visualize the protein-protein interaction and provide spatial and temporal information in living and intact cells with the unique advantages over any other methods, such as the electrophoresis-based systems, the two-hybrid system, mass spectrometry (MS) and immune affinity-based methods.²⁰⁻²² However, BiFC and autofluorescent translocation biosensor techniques usually require a reporter such as the conjugate fluorescent proteins, it's time-consuming, expensive and complicated.⁵ Hence, it is an urgent challenge to develop affordable and straightforward toolkit to visualize and detect this interaction.

For the past few years, fluorescent probes have been widely applied for detecting as well as visualization the biotargets. Compared with BiFC and autofluorescent translocation biosensor techniques, the small-molecule fluorescent probes are more convenient and low cost, especially for the "off-on" mechanism, which disclosed many superiorities^{2,5,23-26} in detecting specific proteins effectively with high signal-to-background ratios.²⁷ Therefore, it is still a thought-provoking task to develop small-molecule fluorescent probes for protein-protein interaction such as p53-MDM2 protein-protein interaction.

In our previous works, we obtained a series of effective fluorescent probes for the p53-MDM2 PPI.²⁵ However, these probes still have some defects, such as the weak fluorescence intensity. To address these issues, we endeavored to find more suitable probes. Recently, Tan group reported a number of turn-on fluorescent probes showed stronger fluorescence intensity in hydrophobic surroundings.²⁸ We chose the fluorophore 4-sulfamoyl-7-aminobenzoxadiazole (SBD) which has relative fluorescent properties as the recognition moiety in an aliphatic spacer. We chose acyl chloride **8** as the pharmacophore, in our previous study, we found that compounds with imidazoline scaffold had excellent binding affinity to MDM2 protein,¹⁴ the structure of pharmacophore is optimized based on the structure of Nutlin-3.^{14,29} Therefore, three environment-sensitive fluorescent probe **9-11** applied into detecting and visualization wild-type p53-MDM2 PPI were well designed, synthesized as well as evaluated. Furthermore, we also applied the probes into A549 and NCI-H1299 tumor tissue slices imaging, the fluorescence images in tissue sections are in line with the results in living cell lines. Our probes showed particular selectivity as the p53-

MDM2 interaction inhibitor and could be used into detecting and imaging the wild-type p53-MDM2 interaction.



Scheme 1. The design strategy of fluorescent probe **9-11**.

Experimental Section

Materials and instruments. General chemicals available from commercial sources and used as received without further purified. ¹H NMR and ¹³C NMR were recorded on a Bruker 400 MHz/600 MHz NMR spectrometer. Fluorescence spectra and absorption spectra were tested by the Bio Tek Instruments microplate reader. Fluorescence imaging of cells was performed on the Zeiss Axio Observer A1 fluorescence microscope. Quantum yields of probes **9-11** were measured by HitachiF-2500 fluorescent spectrometer, Shimadzu UV-2401PC UV-visible spectrometer and WAY-2S Abbe refractometer. Analytical HPLC was performed on Agilent Technologies 1260 Series using a C18 reversed phase column (250 x 4.60mm, Phenomenex). IHC and tissue images was performed on OLYMPUS VS120, Flow cytometry analyzed by the Beckman Cell Counter.

Docking study for probe 10 with MDM2. Follow the previous reports,^{2,30} The initial three dimensional geometric coordinates of the X-ray crystal structure of MDM2 (PDB code: 1T4E) was downloaded from the Protein Data Bank (<http://www.pdb.org/pdb/home/home.do>). Then, we used GOLD 5.1 with GoldScore fitness function to dock probe **10** into its targets for testing the binding conformation of the complex.

Synthesis. In the present research, probe **9-11** to detect p53-MDM2 PPI (**Scheme 1**) are developed based on the docking model of probes complex with MDM2 protein (PDB:1T4E) (**Figure 1**). The synthetic route of probe **9-11** are depicted in **Scheme 2**. Further details of the synthesis can be found in the **Supporting Information**.

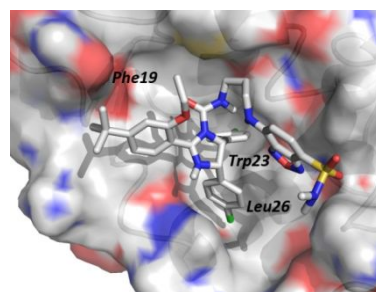
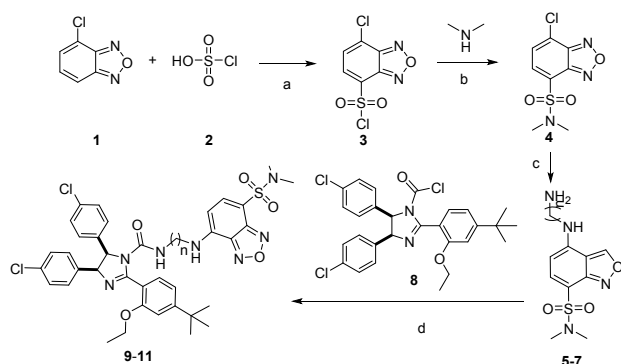


Figure 1. Docking mode of probe-10 with MDM2.



Scheme 2. Synthetic routes of fluorescent probes **9-11**. (a) 120–130 °C, 6 h, 71.0%; (b) Triethylamine, r.t., 0.5 h; dimethylamine hydrochloride, tetrahydrofuran, 1 h, 0 °C, 43.7%; (c) Acetonitrile, 60 °C, 6 h, 92.3%; (d) Triethylamine, DCM, r.t., 30 min, 79.6%.

Fluorescence spectroscopy test. The spectroscopic properties of probes **9-11** were measured at a final concentration of 5 μM diluted with PBS (pH = 7.4) by BioTek multiscan spectrum, respectively. More details of the spectroscopic properties of probe **9-11** can be found in the **Supporting Information**.

MDM2 binding affinity assay. The fluorescence polarization (FP) assay as described previously reports,^{2,30,31} The FP values were read on BioTek (Winooski, VT, USA) Synergy H4 with the filters (Ex: 485 nm and Em: 535 nm). More detail procedures are showed in the **Support Information**.

In vitro anti-proliferative assay. We investigated the cytotoxicity of probes **9-11** and the Nutlin-3 by the CCK-8 method. We select A549 (wild-type p53) and H1299 (p53 null) cell lines to test the cytotoxicity of probe **9-11**. 5×10^3 cells per well were placed in 96-well plates with 100 μL DMEM culture medium (include 10% fetal bovine serum) and then cultured 37 °C in a humidified 5% CO_2 atmosphere overnight. Subsequently, the probes or Nutlin-3 were added to the wells at different concentrations (a series 2-fold dilutions among 3.125–100 μM), and then incubated for another 48 h. Then, follow the protocol of CCK-8, the absorbance value of each well was recorded by BMG microplate reader. The IC_{50} valuable of each probe was calculated by the GraphPad Prism 5.0 software. More details can be found in the **supporting informations**.

Fluorescence microscopy imaging. A549 (wild-type p53) and H1299 (p53 null) cell lines were chosen for the fluorescence imaging. When the cells were in the proliferation period, these two types of cells were transferred to the confocal dish and cultured overnight. Then, the probes **9-11** were further diluted with DMEM medium free fetal bovine serum at a final concentration of 5 μM and co-staining with the nuclear dye Hoechst 33342 500 nM. Subsequently, probes were incubated with A549 and NCI-H1299 cells at 37 °C for 15 min, respectively. The A549 cell line were also performed by commercial

available p53-MDM2 inhibitor (100 μM Nutlin-3) as the positive control incubation together with 5 μM each probe at the same conditions. Then the fluorescence imaging in living A549 and NCI-H1299 cell lines were obtained on a Zeiss Axio Observer A1 fluorescent microscope. The backgrounds of all the images were adjusted by Image J software. Objective lens: 63 \times .

Flow cytometry analysis. The flow cytometry test was performed on A549 cell line. When the cells were in the proliferation period, cells were collected and washed with $1 \times$ PBS for three times. Probes **9-11** was added at a final concentration of 5 μM , respectively or together with the positive control (100 μM Nutlin-3) into the flow tubes with 300 μL PBS and 1×10^5 cells each tube. After incubation for about 30 min at 37 °C in dark environment, the samples were analyzed by Beckman Cell Counter.

Western Blot. The protein level of p53 and MDM2 in A549 cancer cell line (wild-type p53) were detect by western blot. When A549 cell reaching 60–70% confluency, the cells were harvested and transferred into 6 wells plate (Corning), after cultured for 12h, probe **9-10** (10 μM , respectively) and Nutlin-3 (5 μM) were added in different well. After 24 h drugs treatment, cells were collected. Then, the cells were lysed by RIPA Lysis and Extraction Buffer and the protein concentration was quantitated by BCA Protein Assay Kit. Then, the protein extract was denatured and run on 12% SDS polyacrylamide gels. Gels were transferred to 0.45 μM PVDF membranes. The membranes were blocked with 5% milk buffer (5% nonfat dry milk in TBS/0.1% tween-20) for 2 h at room temperature and washed three times by TBST (each time for 5 min). The membranes were incubated with the primary antibody specific for p53 (Abcam, ab7757; 1:800), MDM2 (Abcam, ab16895; 1:600), GAPDH (Abcam, ab181602; 1:10000) overnight at 4 °C and washed three times by TBST. Next, the PVDF membranes were incubated with a secondary antibody (Abcam, ab216777; 1:10000) carry out 2 h incubation at room temperature. After washing by TBST, Each protein was detected by BeyoECL Plus (Beyotime Biotechnology, P0018S, Shanghai, China) with ChemiDoc XRS imaging system (Bio-Rad, Hercules, CA), and the protein levels were quantitated by the gray values of the bands by the Image J software.

Immunohistochemical analysis of A549 and NCI-H1299 tumor tissue slices. According to the protocol of Immunohistochemistry, tissue slices were deparaffinized in xylene, then rehydration in graded alcohols, after antigen repaired by All-purpose Powerful Antigen Retrieval Solution (Beyotime Biotechnology, P0088, Shanghai, China) at 95–100 °C for 20 min, the slices were incubation with primary antibodies Anti-p53 antibody [E26] ab32389 (1:100, abcam) overnight at 4 °C. And then were incubated with secondary antibody goat anti-mouse Ig G and goat antibody rabbit Ig G polymer (Gene Tech, GK600505, Shanghai, China) at room temperature for 15 min, followed by staining with DAB at room temperature

for 5 min. Finally, tumor slices were washed, and then counterstained with hematoxylin, after dehydration by gradient ethanol, mounted under cover slips by neutral gum. The slices were captured by the OLYMPUS VS120. Objective lens: 40 \times .

Imaging analysis of paraffin embedded A549 and NCI-H1299 tumor tissue slices. The stock solution (10 mM) of probes was diluted in Krebs buffer (pH =7.4) to obtain 10 μ M probe solutions. After tissue sections were antigen repaired, the slices were incubation with probe **9-11** overnight at 4 $^{\circ}$ C, and aslo set A549 tumor slice incubated with probe and nutlin-3, respectively. The slices were captured by the OLYMPUS VS120. Objective lens: 40 \times .

Results and Discussion

Spectroscopic Properties of Probes. As shown in the Table 1 and Figure S1, all the probe **9-11** possessed efficient fluorescent properties, the relatively quantum yield of probe **9-11** all > 40% in DMSO, and >10% in the PBS, revealed that the probe **9-11** possessed the environment-sensitive turn-on mechanism in different solvent environment.

Table 1. Photophysical properties of probes **9-11**

Compound	λ_{\max} (nm)	λ_{ex} (nm)	λ_{em} (nm)	Φ (%)	
				PBS	DMSO
Probe 9	420	425	565	13.35	55.96
Probe 10	443	450	580	10.81	41.55
Probe 11	450	450	575	11.67	40.15

MDM2 binding affinity assay. In this assay test, Nutlin-3 as the positive control, the K_i value is 198 nM. We found that probe **10** and **11** indicated reasonable binding activity with K_i values of 126 and 74.8 nM, respectively (Table 2 and Figure S2), probe **10** and **11** showed higher potency than the reference compound.

Fluorescent Properties of Probes Combined with MDM2 Proteins and Nonspecific Protein BSA. All the probes were designed for MDM2 protein, The result displayed that there is little change of FP value with MDM2 protein at different concentration, and the parameter setting are emission wavelength: 535 nm and excitation wavelength: 485 nm (Table S1). Furthermore, we also measured the fluorescence properties of probe **9-11** with BSA (bovine serum albumin), for BSA could be formed non-specific binding with probe. The assay results indicated that a slight interaction in probe **9-11** with BSA (Figure S3).

Cytotoxicity Assay. The CCK-8 method was used to investigated the cytotoxicity of probe **9-11** and Nutlin-3. H1299 and A549 cell lines were selected to test the cytotoxicity of probe **9-11**. Overall, our probes exposed low cytotoxicity (Table 2). These antiproliferative results

proved that probe **9-11** can be applied into detecting as well as visualization the p53-MDM2 PPI in living cells.

Table 2. Biological data of probes **9-11**

Compound	K_i (nM)	IC_{50} (μ M)	
		A549	H1299
Probe 9	993 \pm 92.7	81.1 \pm 13.0	>100
Probe 10	126 \pm 26.9	55.1 \pm 2.58	55.6 \pm 2.44
Probe 11	74.8 \pm 10.7	98.0 \pm 0.62	>100
Nutlin-3	198 \pm 37.1	5.65 \pm 0.66	20.9 \pm 3.01

Fluorescent Imaging. Considering the reasonable binding activity of probes **9-11** and low cytotoxicity, we evaluated probes **9-11** for detecting the p53-MDM2 PPI in A549 cells as well as NCI-H1299 by Zeiss Axio Observer A1 microscope. The experimental results exhibited that the fluorescence intensity is stronger in the p53 wild-type cell line A549 than the p53 null cell line NCI-H1299 (Figures 2-4). When co-staining with the nuclear dye Hoechst 33342, the results displayed that the p53-MDM2 interaction mainly located in the cytoplasm, which is in line with the previous reports^{2,19,20} that MDM2 is mainly located in the cytoplasm. We also chose Nutlin-3 as the control to examine whether these probes could bind with p53-MDM2, we incubated 100 μ M Nutlin-3 with 5 μ M probes **9-11** in the p53 wild-type A549 cell line, respectively. The result revealed that Nutlin-3 could decrease the fluorescence intensity compared with incubate probes alone. The results (Figure 2-4) proved that our probes had binding with p53-MDM2, so that can be applied into detecting the wild-type p53-MDM2 interaction in the cell level.

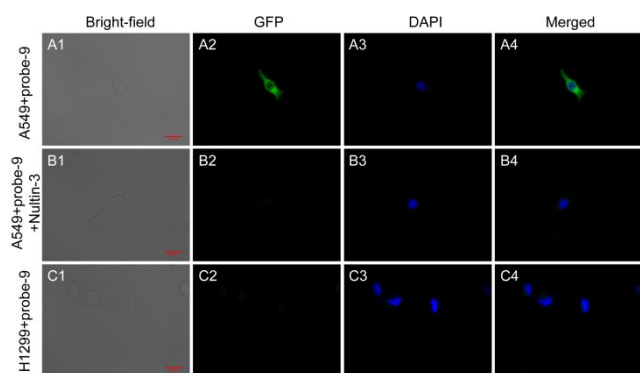


Figure 2. Fluorescence microscopic imaging of A549 cells and NCI-H1299 cells incubated with 5 μ M probe **9**. A1, B1 and C1- bright field; A2, B2 and C2-GFP channel; A3, B3 and C3 were stained by the nuclear dye Hoechst 33342, and A4, B4 and C4 are the merged images. A549 (A) and NCI-H1299 (C) cells were incubated with 5 μ M probe **9**; (B) is the p53 wide-type cell line A549 incubating 5 μ M probe **9** with 100 μ M Nutlin-3. Scale bar = 67 μ m.

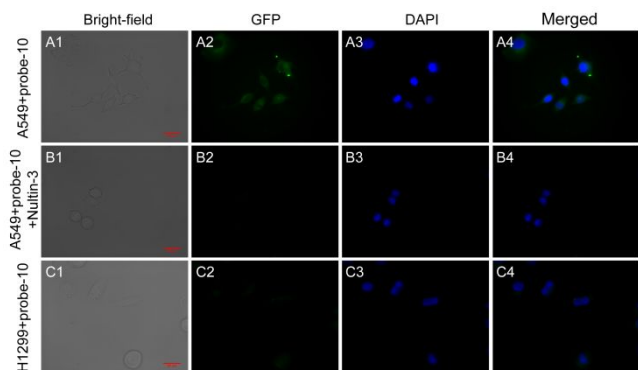


Figure 3. Fluorescence microscopic imaging of A549 cells and NCI-H1229 cells incubated with 5 μ M probe 10. A1, B1 and C1- bright field; A2, B2 and C2-GFP channel; A3, B3 and C3 were stained by the nuclear dye Hoechst 33342, and A4, B4 and C4 are the merged images. A549 (A) and NCI-H1229 (C) cells were incubated with 5 μ M probe 10; (B) is the p53 wide-type cell line A549 incubating 5 μ M probe 100 μ M 10 with Nutlin-3. Scale bar = 67 μ m.

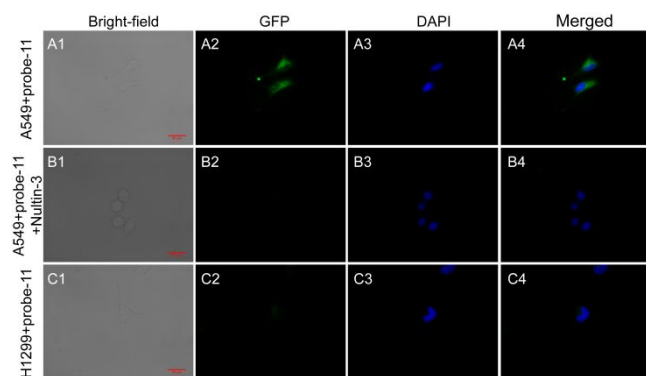


Figure 4. Fluorescence microscopic imaging of A549 cells and NCI-H1229 cells incubated with 5 μ M probe 11. A1, B1 and C1- bright field; A2, B2 and C2-GFP channel; A3, B3 and C3 were stained by the nuclear dye Hoechst 33342, and A4, B4 and C4 are the merged images. A549 (A) and NCI-H1229 (C) cells were incubated with 5 μ M probe 11; (B) is the p53 wide-type cell line A549 incubating 5 μ M probe 11 with 100 μ M Nutlin-3. Scale bar = 67 μ m.

Flow Cytometry (FCM) Assay. The FCM method was used to measure the binding ability of probe 9-11 or/and Nutlin-3 in A549 cell line. The result showed that the fluorescence intensity of probe 9-11 to the A549 cells was more stronger than the A549 cells co-incubated by probes with Nutlin-3 (Figure 5). And proved that nutlin-3 could decreased the binding ability of probe 9-11 in A549 cell line. These FCM results are consistent with the fluorescence microscopic imaging assay in the A549 living cell lines.

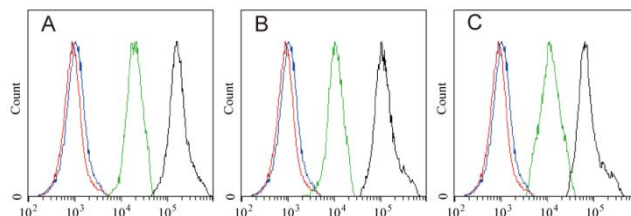


Figure 5. The fluorescence intensity of 5 μ M probe 9-11 or/and 100 μ M nutlin-3 in A549 cell line measured by FCM (Red: negative control; Blue: Nutlin-3; Black: probe 9-11; Green: Nutlin-3 was incubated with probe 9-11). A-C are probe 9, probe 10 and probe 11, respectively.

Detect the protein level of p53 and MDM2 in A549 cell line by western blot. We examined whether probes 9-11 could inhibit the p53-MDM2 interaction in the A549 cell line by Western Blot. Interestingly, all the probes exposed a same up-regulation of p53 and MDM2 level in A549 cells as positive control (Figure 6). The qualification result demonstrated that probes 2-3 can increase the expression levels of p53 than Nutlin-3 (Figure 6B). Therefore, these probes could induce apoptosis of tumor cells, inhibit the tumor cell proliferation.

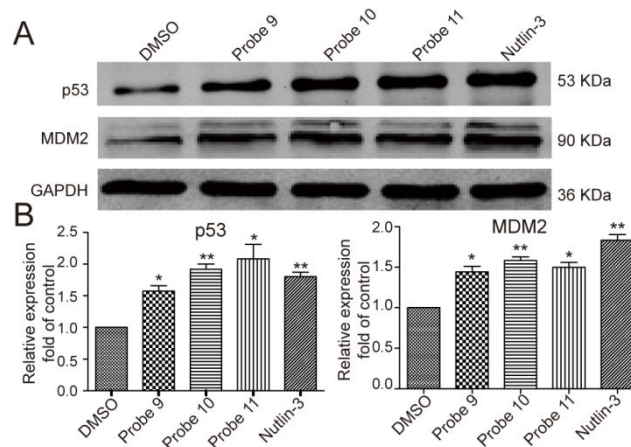


Figure 6. Cellular activity for probe 9-11 for the p53 pathway activation detected by Western Blot (A549 cell lines). A: the western blot images of each groups; B: the qualification of the protein levels by the gray values of the bands A by the Image J, the concentration of Nutlin-3 is 5 μ M, and the concentrations of probe 9-11 is 10 μ M, respective. Data were analyzed by paired t test, * p <0.05, ** p <0.01 vs. DMSO group.

Hematoxylin-eosin (HE) and Immunohistochemical (IHC) Experiments. HE staining was provided by Qilu Hospital of Shandong University. The HE staining results indicated that the A549 and H1299 tumor slices exhibited pathological condition. In order to detected the protein expression level of p53 in tissue, we conducted the IHC experiment, after the tissue incubated with primary antibodies Anti-p53 antibody and the second antibody, the IHC imaging results (Figure 7) proved that A549 tumors exhibited the highest immunostaining, whereas NCI-H1299 tumors showed weak staining for anti-p53.

This results in accordance with the fact that A549 is the p53 wide-type cell line and that NCI-H1299 is the p53 null cell line. Therefore, the A549 and H1299 tumor tissue slices could be well applied into tissue slice imaging assay.

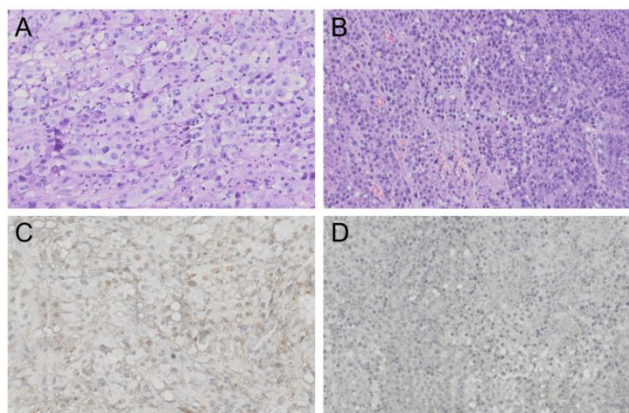


Figure 7. HE staining and IHC of A549 and NCI-H1299 tumor slices. A549 tumor exhibited the strongest immunostaining for anti-p53. A: A549 tumor slices HE staining; B: NCI-H1299 tumor slices HE staining; C: the A549 tumor slice incubated with primary antibodies Anti-p53 antibody; D: the NCI-H1299 tumor slice incubated with primary antibodies Anti-p53 antibody. OLYMPUS VS120 performed the images with a 10 \times objective lens.

We also evaluated whether probe **9-11** can selectively detect wild-type p53-MDM2 interaction in the tumor slices. After antigen repaired, the slices were incubation with probes overnight at 4 $^{\circ}$ C. The imaging results (**Figure 8**) proved that our probes could significantly labeled in the A549 tumor slice; while staining is lower in the NCI-H1299 tumor section and A549 tumor slice co-incubated with probe and Nutlin-3, which is in accordance with the fluorescence image assay in living cells. The tissue slice imaging results revealed that our probe **9-11** can be applied into cancer diagnosis in pathophysiological condition in future.

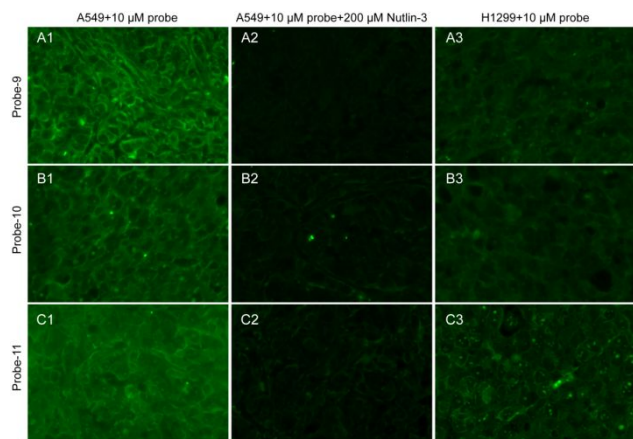


Figure 8. Imaging on tumor slices of probe **9-11**. A1, B1 and C1 were A549 tumor slices incubated with 10 μ M probe only; A2, B2 and C2 were A549 tumor incubated

with 10 μ M probe and 200 μ M Nutlin-3; A3, B3 and C3 were NCI-H1299 tumor incubated with 10 μ M probe. OLYMPUS VS120 performed the images with a 20 \times objective lens.

Conclusion

In this study, we have designed a novel class of non-peptide small-molecule MDM2 inhibitors with excellent fluorescent properties for detecting and imaging the p53-MDM2 interaction. These three probes could bind to the hydrophobic domain of p53 on MDM2 surface by an environment-dependent turn-on mechanism. Compared with other imaging method, such as immunofluorescence and fluorescent protein-based techniques, the small-molecule fluorescent probe is affordable, convenient, and rapid. After multiple bioactivity evaluations in living cell lines and tumor tissues, three fluorescent probes **9-11** exhibited potent affinities and particularly sensitive for the wild-type p53-MDM2 interaction. In summary, the novel class of non-peptide small-molecule MDM2 inhibitors may lead to the development of an entirely new type of anticancer drugs and drug screening. The small-molecule environment-sensitive fluorescent probes have an advance development, and look forward to applying into human clinical in the future.

ASSOCIATED CONTENT

Supporting Information

More detail synthesis experiment procedures, NMR and MS spectra. The Supporting Information is available free of charge on the ACS Publications website at DOI: 10.1021/.

AUTHOR INFORMATION

Corresponding Author

*Tel/Fax: +86-531-8838-2076. E-mail: mli@sdu.edu.cn; shengcq@hotmail.com.

Author Contributions

The final manuscript was approved by all authors.

Conflict of Interest Disclosure

The authors declare no competing financial interest.

ACKNOWLEDGMENT

This work was supported by grants from the Shandong Natural Science Foundation (No. ZR2018ZC0233), the Taishan Scholar Program at Shandong Province, the Qilu/Tang Scholar Program at Shandong University, and the Key Research and Development Project of Shandong Province (No. 2017CXGC1401).

REFERENCES

- (1) Wang, W.; Hu, Y. Small molecule agents targeting the p53-MDM2 pathway for cancer therapy. *Med. Res. Rev.* **2012**, *32*, 1159-1196.
- (2) Liu, Z.; Miao, Z.; Li, J.; Fang, K.; Zhuang, C.; Du, L.; Sheng, C.; Li, M. A fluorescent probe for imaging p53-MDM2 protein-protein interaction. *Chem. Biol. Drug Des.* **2015**, *85*, 411-417.

- (3) Levine, A. J. p53, the cellular gatekeeper for growth and division. *Cell*. **1997**, *88*, 323-331.
- (4) Vogelstein, B.; Lane, D.; Levine, A. J. Surfing the p53 network. *Nature*. **2000**, *408*, 307-310.
- (5) Liu, T.; Jiang, Y.; Liu, Z.; Li, J.; Fang, K.; Zhuang, C.; Du, L.; Fang, H.; Sheng, C.; Li, M. Environment-sensitive turn-on fluorescent probes for p53-MDM2 protein-protein interaction. *Med.Chem.Comm.* **2017**, *8*, 1668-1672.
- (6) Shangary, S.; Wang, S. Targeting the MDM2-p53 interaction for cancer therapy. *Clin. Cancer Res.* **2008**, *14*, 5318-5324.
- (7) Teodoro, J. G.; Evans, S. K.; Green, M. R. Inhibition of tumor angiogenesis by p53: a new role for the guardian of the genome. *J. Mol. Med (Berl)*. **2007**, *85*, 1175-1186.
- (8) Wu, X.; Bayle, J. H.; Olson, D.; Levine, A. J. The p53-mdm-2 autoregulatory feedback loop. *Genes Dev.* **1993**, *7*, 1126-1132.
- (9) Haupt, Y.; Maya, R.; Kazaz, A.; Oren, M. Mdm2 promotes the rapid degradation of p53. *Nature*. **1997**, *387*, 296-299.
- (10) Momand, J.; Zambetti, G. P.; Olson, D. C.; George, D.; Levine, A. J. The mdm-2 oncogene product forms a complex with the p53 protein and inhibits p53-mediated transactivation. *Cell*. **1992**, *69*, 1237-1245.
- (11) Chen, J.; Marechal, V.; Levine, A. J. Mapping of the p53 and mdm-2 interaction domains. *Mol. Cell. Biol.* **1993**, *13*, 4107-4114.
- (12) Freedman, D. A.; Levine, A. J. Nuclear export is required for degradation of endogenous p53 by MDM2 and human papillomavirus E6. *Mol. Cell. Biol.* **1998**, *18*, 7288-7293.
- (13) Fang, S.; Jensen, J. P.; Ludwig, R. L.; Vousden, K. H.; Weissman, A. M. Mdm2 is a RING finger-dependent ubiquitin protein ligase for itself and p53. *J. Biol. Chem.* **2000**, *275*, 8945-8951.
- (14) He, S.; Dong, G.; Wu, S.; Fang, K.; Miao, Z.; Wang, W.; Sheng, C. Small Molecules Simultaneously Inhibiting p53-Murine Double Minute 2 (MDM2) Interaction and Histone Deacetylases (HDACs): Discovery of Novel Multitargeting Antitumor Agents. *J. Med. Chem.* **2018**, *61*, 7245-7260.
- (15) Kussie, P. H.; Gorina, S.; Marechal, V.; Elenbaas, B.; Moreau, J.; Levine, A. J.; Pavletich, N. P. Structure of the MDM2 oncoprotein bound to the p53 tumor suppressor transactivation domain. *Science*. **1996**, *274*, 948-953.
- (16) Wang, S.; Sun, W.; Zhao, Y.; McEachern, D.; Meaux, I.; Barriere, C.; Stuckey, J. A.; Meagher, J. L.; Bai, L.; Liu, L.; Hoffman-Luca, C. G.; Lu, J.; Shangary, S.; Yu, S.; Bernard, D.; Aguilar, A.; Dos-Santos, O.; Besret, L.; Guerif, S.; Pannier, P.; Gorge-Bernat, D.; Debussche, L. SAR405838: an optimized inhibitor of MDM2-p53 interaction that induces complete and durable tumor regression. *Cancer Res.* **2014**, *74*, 5855-5865.
- (17) Tovar, C.; Graves, B.; Packman, K.; Filipovic, Z.; Higgins, B.; Xia, M.; Tardell, C.; Garrido, R.; Lee, E.; Kolinsky, K.; To, K. H.; Linn, M.; Podlaski, F.; Wovkulich, P.; Vu, B.; Vassilev, L. T. MDM2 small-molecule antagonist RG7112 activates p53 signaling and regresses human tumors in preclinical cancer models. *Cancer Res.* **2013**, *73*, 2587-2597.
- (18) Amaral, J. D.; Herrera, F.; Rodrigues, P. M.; Dionisio, P. A.; Outeiro, T. F.; Rodrigues, C. M. Live-cell imaging of p53 interactions using a novel Venus-based bimolecular fluorescence complementation system. *Biochem Pharmacol.* **2013**, *85*, 745-752.
- (19) Lee, K. B.; Hwang, J. M.; Choi, I. S.; Rho, J.; Choi, J. S.; Kim, G. H.; Kim, S. I.; Kim, S.; Lee, Z. W. Direct monitoring of the inhibition of protein-protein interactions in cells by translocation of PKCdelta fusion proteins. *Angew. Chem. Int. Edit.* **2011**, *50*, 1314-1317.
- (20) Knauer, S. K.; Stauber, R. H. Development of an autofluorescent translocation biosensor system to investigate protein-protein interactions in living cells. *Anal. Chem.* **2005**, *77*, 4815-4820.
- (21) Ngounou Wetie, A. G.; Sokolowska, I.; Woods, A. G.; Roy, U.; Loo, J. A.; Darie, C. C. Investigation of stable and transient protein-protein interactions: Past, present, and future. *Proteomics.* **2013**, *13*, 538-557.
- (22) Kerppola, T. K. Bimolecular fluorescence complementation (BiFC) analysis as a probe of protein interactions in living cells. *Annu. Rev. Biophys.* **2008**, *37*, 465-487.
- (23) Ma, Z.; Lin, Y.; Cheng, Y.; Wu, W.; Cai, R.; Chen, S.; Shi, B.; Han, B.; Shi, X.; Zhou, Y.; Du, L.; Li, M. Discovery of the First Environment-Sensitive Near-Infrared (NIR) Fluorogenic Ligand for alpha1-Adrenergic Receptors Imaging in Vivo. *J. Med. Chem.* **2016**, *59*, 2151-2162.
- (24) Liu, J.; Tian, C.; Jiang, T.; Gao, Y.; Zhou, Y.; Li, M.; Du, L. Discovery of the First Environment-Sensitive Fluorescent Probe for GPR120 (FFA4) Imaging. *ACS Med. Chem. Lett.* **2017**, *8*, 428-432.
- (25) Liu, Z.; Jiang, T.; Wang, B.; Ke, B.; Zhou, Y.; Du, L.; Li, M. Environment-Sensitive Fluorescent Probe for the Human Ether-a-go-go-Related Gene Potassium Channel. *Anal. Chem.* **2016**, *88*, 1511-1515.
- (26) Liu, T.; Dong, G.; Xu, F.; Han, B.; Fang, H.; Huang, Y.; Zhou, Y.; Du, L.; Li, M. Discovery of Turn-On Fluorescent Probes for Detecting Bcl-2 Protein. *Anal. Chem.* **2019**, *91*, 5722-5728.
- (27) Lavis, L. D.; Raines, R. T. Bright ideas for chemical biology. *ACS Chem. Biol.* **2008**, *3*, 142-155.
- (28) Zhuang, Y. D.; Chiang, P. Y.; Wang, C. W.; Tan, K. T. Environment-sensitive fluorescent turn-on probes targeting hydrophobic ligand-binding domains for selective protein detection. *Angew. Chem. Int. Edit.* **2013**, *52*, 8124-8128.
- (29) Secchiero, P.; Bosco, R.; Celeghini, C.; Zauli, G. Recent advances in the therapeutic perspectives of Nutlin-3. *Curr. Pharm. Des.* **2011**, *17*, 569-577.
- (30) Zhuang, C.; Miao, Z.; Zhu, L.; Dong, G.; Guo, Z.; Wang, S.; Zhang, Y.; Wu, Y.; Yao, J.; Sheng, C.; Zhang, W. Discovery, synthesis, and biological evaluation of orally active pyrrolidone derivatives as novel inhibitors of p53-MDM2 protein-protein interaction. *J. Med. Chem.* **2012**, *55*, 9630-9642.
- (31) Ding, K.; Lu, Y.; Nikolovska-Coleska, Z.; Qiu, S.; Ding, Y.; Gao, W.; Stuckey, J.; Krajewski, K.; Roller, P. P.; Tomita, Y.; Parrish, D. A.; Deschamps, J. R.; Wang, S. Structure-based design of potent non-peptide MDM2 inhibitors. *J. Am. Chem. Soc.* **2005**, *127*, 10130-10131.

Table Of Content

